Simulations of a Fox-Rabies Epidemic on an Island Using Space-Time Finite Elements

Gwen A. Gardner, Leslie R. T. Gardner, and John Cunningham
School of Mathematics, University of Wales, UCNW, Bangor, Gwynedd LL57 1UT, U.K.

Z. Naturforsch. **45c**, 1230–1240 (1990); received December 27, 1989

Epidemiology, Rabies, Reaction-Diffusion Equation, Finite Elements

The two-dimensional reaction diffusion equations for the spread of rabies in a logistically growing fox population are solved numerically. The method, based upon Galerkin's approach, uses space-time finite elements. The numerical model is shown, quantitatively, to possess the essential features of earlier one and two-dimensional models and to reproduce the values of field data accurately. A more realistic illustration of the use of the model, a study of the spread of rabies over the Isle of Anglesey, is then discussed.

Introduction

It is thought that all mammals are susceptible to rabies which is a directly transmitted viral infection of the central nervous system [1–4]. This infectious disease has distressing and often hideous clinical symptoms, and once these symptoms have manifested themselves death is virtually certain [5, 6].

In the major European epidemics recorded over the past few centuries the dog has acted as the main host and primary transmitter of the infection to man [1, 5]. The present epidemic in Central Europe originated in Poland in about 1939 and is characterized by a high incidence of the red fox *Vulpes vulpes*. In 1979 it was found that 70% of all reported cases of animal rabies were in this species [7]. The present epidemic of rabies has moved steadily westwards across Europe at a rate of between 30–60 km per year. Its progress has been temporarily slowed by unsuitable terrains such as high mountains, wide rivers, lakes and autobahns, but never stopped. In the wake of the leading epidemic transient there follow lesser pulses of the disease giving rise eventually to an endemic state in which a low level of rabies exists in a reduced total fox population, with small periodic resurgences of the disease every 3–4 years. Although other species can be involved in the spread of rabies it is thought that the main carrier in the present epidemic in Europe is the red fox. So here we will assume that the spread of the disease is intimately linked into the ecology of the fox populations.

The wave front of the European epizootic has reached Paris and is close to the northern ports of France despite attempts to impede its progress by the use of slaughter or vaccination policies. It now seems inevitable that rabies will be introduced into Britain by an imprudent traveller taking in an infected animal.

It has been observed that the speed of spread of rabies is more rapid the higher the fox density and the higher the density of domestic pets the more likely is the disease to be transmitted to them and hence to man. The appearance of rabies will thus pose a very serious problem in Britain since the population densities of both urban foxes and domestic pets, such as dogs and cats, are higher than those in mainland Europe [8, 9].

Over the years, rabies has fascinated research workers; consequently there have been many studies of the rabies problem [8–10] and more recently numerical models for the spread of rabies have been developed [11–17].

In previous papers [14–17] we have set up and used numerical models based on finite difference and finite element techniques to study the mechanisms by which rabies spreads and have successfully modelled the velocity of the infective pulse, the endemic levels of infectives and susceptibles and the period of the post epidemic recurrences.

In the present paper we set up a space-time finite element solution over a rectangular area. Initially we validate the model and seek to establish whether there are any significant differences between the predictions of the earlier models and this 2D model either in the speed of the spread or in its charac-

Reprint requests to Dr. G. A. Gardner.

Verlag der Zeitschrift für Naturforschung, D-7400 Tübingen
0341–0382/90/1100–1230 $ 01.30/0

teristics. Finally a simulation of the spread of rabies over a rectangular region, modelling the Isle of Anglesey, is set up and discussed.

The Governing Differential Equations

Foxes are territorial animals. Their territories divide the countryside up into non-overlapping regions and healthy foxes tend to remain within their own territories. Rabies is transmitted in saliva by bite and the rate of increase of infective foxes is assumed to be proportional to the number of contacts between rabid and healthy foxes. Once rabid, foxes never recover and so the death rate from rabies is assumed proportional to the number of infective foxes. As the infection is severely debilatating, and of short duration, it is assumed that infected foxes do not contribute to the reproduction process. Also, rabid foxes lose their sense of territoriality and tend to disperse across the countryside. These assumptions lead to the governing equations for the fox-rabies problem

$$\frac{\partial S}{\partial t} = -cIS - aS(I+S) + aS_0 S$$

$$\frac{\partial I}{\partial t} = cIS - aI(I+S) - rI + d\left(\frac{\partial^2 I}{\partial x^2} + \frac{\partial^2 I}{\partial y^2}\right)$$

where $S(x,y,t)$ is the seasonally averaged susceptible fox density, $I(x,y,t)$ that for the infectives, and a, c, r, d and S_0 are positive biological parameters.

The cIS term in each equation represents the effect of contacts between susceptible and infected foxes and measures the decrease in susceptibles and the consequent increase in infectives, $c>0$ is the contact parameter. The term $aS(S+I)$ in the first equation and $aI(S+I)$ in the second show the effect of competition for resourses between each class and the total population, $a>0$ measures its effectiveness. Increase of the population due to births is allowed for by the term aS_0S in the first equation, where aS_0 is the birth rate and the decrease, through death from rabies, by the term rI in the second equation; $r>0$ is the death rate. The death rate of non rabid foxes is accounted for by a modification of the birth rate. Finally, the diffusion term in the second equation, where d is the uniform, isotropic, constant diffusion coefficient, represents the dispersal of infective foxes due to a loss of a sense of territoriality engendered by the disease.

A normalization of these equations, based on the biology of the problem, which effectively reduces the number of free parameters, has been previously described [14–16]. Those normalized, two parameter, equations can, for the two dimensional case, be written

$$\frac{\partial S}{\partial t} = S[b - (1+b)I - bS] \tag{1}$$

$$\frac{\partial I}{\partial t} = I[(1-b)S - r - bI] + \frac{\partial^2 I}{\partial x^2} + \frac{\partial^2 I}{\partial y^2} \tag{2}$$

over the region $0<x<\ell_x$, $0<y<\ell_y$, where $S(x,y,t)$ is the susceptible fox density and $I(x,y,t)$ the density of infectives. The population densities are scaled to the carrying capacity of the region (the number of foxes the habitat can support) which is assumed uniform and constant.

In these simulations both time and distance are scaled to condense the biological data into two computational parameters r and b which reflect the following assumptions.

1) The mean lifetime of an infected fox is 35 days (30 days latent and 5 days infectious/rabid);

2) contacts between healthy fox families occur on the average every 4 or 5 days but only contacts made during the 5 days rabidity are potentially infectious.

3) Not all contacts result in infection but rabidity increases activity and we have assumed that effective contacts are approximately double the number which would result from a direct application of assumption 2.

4) The mean size of a fox territory is 5 km^2 corresponding to a fox density of 1 fox km^{-2}; this is believed to be reasonable in Continental Europe although territory sizes vary from 2.5 km^2 to 16 km^2 depending on the availability of resources; U K densities are thought to be somewhat higher.

5) Rabid symptoms result in loss of sense of territoriality after about 30 days.

6) Diffusive spread is due to a combination of loss of territoriality and seasonal migration of latent dog foxes (incubating rabies).

We assume that there is zero flow through any boundary and so take as boundary conditions

$$\frac{\partial S}{\partial x} = \frac{\partial I}{\partial x} = 0 \quad x = 0, \ell_x \tag{3}$$

$$\frac{\partial S}{\partial y} = \frac{\partial I}{\partial y} = 0 \quad y = 0, \ell_y \tag{4}$$

The Numerical Solution

Eqns. (1) and (2) are obviously of different types since (2) contains spatial derivatives which imply a spatial dependence of the solution while Eqn. (1) does not. We shall therefore use a different approach for the solution of each.

We apply Galerkins method [18] to Eqn. (1) for a finite element in time of length Δt using as weight function $W = 1$ and

$$S = S_j + \tau\,\Delta S_j,\ I = I_j + \tau\,\Delta I_j,\ t = t_0 + \tau\,\Delta t, \quad (5)$$

where S_j and I_j are the nodal values and ΔS_j and ΔI_j are the changes in these values over the time element Δt giving

$$\int_0^1 \left[\frac{\Delta S_j}{\Delta t} - (S_j + \tau\Delta S_j)\,[b - (1+b)\,(I_j + \tau\Delta I_j) - b\,(S_j + \tau\Delta S_j)]\right] d\tau = 0.$$

Integrating with respect to τ, and ignoring second order quantities, such as the products $\Delta S_j\ \Delta I_j$, leads to the incremental equation

$$\Delta S_j = S_j \left[\frac{b - (1+b)\,I_j - b\,S_j}{\frac{1}{\Delta t} - \frac{b}{2} + \left(\frac{1+b}{2}\right) I_j + bS_j}\right] \quad (6)$$

for the changes in S_j, where $S_j = S_j^n$ and $I_j = I_j^n$ are the nodal values at time level $t = n\,\Delta t$, so that the nodal values at time level $t = (n+1)\,\Delta t$ are given by

$$S^{n+1} = S^n + \Delta S \quad (7)$$

where S is the vector of all nodal values for the susceptibles.

Turning now to Eqn. (2) we apply a space-time Galerkin approach [18]. With weight function W the weak form of Eqn. (2) is

$$F_2 = \int_0^{\Delta t}\int_0^{\ell x}\int_0^{\ell y} W\left[\dot{I} - (1-b)\,IS + rI + bI^2 - \frac{\partial^2 I}{\partial x^2} - \frac{\partial^2 I}{\partial y^2}\right] dy\,dx\,dt = 0 \quad (8)$$

where the region of integration is $0 \le x \le \ell x$, $0 \le y \le \ell y$, $0 \le t \le \Delta t$. Integrating the terms involving the second spatial derivatives by parts and applying boundary conditions (3) and (4) we obtain the reduced form

$$F_2 = \int_0^{\Delta t}\int_0^{\ell x}\int_0^{\ell y}\left[W\{\dot{I} - (1-b)\,IS + rI + bI^2\} + \frac{\partial W}{\partial x}\frac{\partial I}{\partial x} + \frac{\partial W}{\partial y}\frac{\partial I}{\partial y}\right] dy\,dx\,dt = 0. \quad (9)$$

For the spatial rectangular element of sides Δx, Δy, with nodes at its corners numbered anticlockwise, starting from the lower left hand corner, the distribution of infectives I^e and susceptibles S^e over the element is given in terms of the nodal values I_j^e, S_j^e by

$$I^e = \sum_{j=1}^{4} N_j\,(I_j^e + \tau\Delta I_j^e),\ S^e = \sum_{j=1}^{4} N_j\,(S_j^e + \tau\Delta S_j^e), \quad (10)$$

where the shape functions N_j are

$$N_j = [(1-\xi)\,(1-\eta),\ \xi(1-\eta),\ \xi\eta,\ \eta(1-\xi)] \quad (11)$$

in terms of local coordinates ξ, η with $0 \le \xi \le 1$, $0 \le \eta \le 1$, and τ is related to time through $t = t_0 + \tau\Delta t$ with $0 \le \tau \le 1$.

Thus if we identify the weight function W with a shape function N_j, use Eqn. (10) and integrate with respect to time we find that a single element's contribution to (9) is

$$F_2^e = \frac{1}{\Delta t}\sum_j C_{ij}^e\,\Delta I_j^e - (1-b)\sum_{j,k} L_{ijk}^e\left(I_j^e\,S_k^e + \frac{1}{2}\,I_j^e\,\Delta S_k^e + \frac{1}{2}\,S_k^e\,\Delta I_j^e\right)$$
$$+ r\sum_j C_{ij}^e\left(I_j^e + \frac{1}{2}\,\Delta I_j^e\right) + b\sum_{j,k} L_{ijk}^e\,(I_j^e\,I_k^e + I_k^e\,\Delta I_j^e) + \sum_j (D_{ij}^e + E_{ij}^e)\left(I_j^e + \frac{1}{2}\,\Delta I_j^e\right) \quad (12)$$

where

$$\left.\begin{aligned} C^e_{ij} &= \int_0^1 \int_0^1 N_i N_j \, d\xi d\eta \, \Delta x \, \Delta y \\ D^e_{ij} &= \int_0^1 \int_0^1 \frac{\partial N_i}{\partial \xi} \frac{\partial N_j}{\partial \xi} \, d\xi d\eta \, \frac{\Delta y}{\Delta x} \\ E^e_{ij} &= \int_0^1 \int_0^1 \frac{\partial N_i}{\partial \eta} \frac{\partial N_j}{\partial \eta} \, d\xi d\eta \, \frac{\Delta x}{\Delta y} \\ L^e_{ijk} &= \int_0^1 \int_0^1 \int_0^1 N_i N_j N_k \, d\xi d\eta \, \Delta x \, \Delta y \end{aligned}\right\} \quad (13)$$

It is convenient to define two associated 4×4 matrices by

$$A^e_{ij} = \sum_k L^e_{ijk} I^e_k, \text{ and } B^e_{ij} = \sum_k L^e_{ijk} S^e_k.$$

These element matrices have been evaluated using the Computer Algebra package REDUCE [19] and are given by

$$C^e_{ij} = \frac{\Delta x \Delta y}{36} \begin{bmatrix} 4 & 2 & 1 & 2 \\ 2 & 4 & 2 & 1 \\ 1 & 2 & 4 & 2 \\ 2 & 1 & 2 & 4 \end{bmatrix} \quad (14)$$

$$D^e_{ij} = \frac{\Delta y}{6 \Delta x} \begin{bmatrix} 2 & -2 & -1 & 1 \\ -2 & 2 & 1 & -1 \\ -1 & 1 & 2 & -2 \\ 1 & -1 & -2 & 2 \end{bmatrix} \quad (15)$$

$$E^e_{ij} = \frac{\Delta x}{6 \Delta y} \begin{bmatrix} 2 & 1 & -1 & -2 \\ 1 & 2 & -2 & -1 \\ -1 & -2 & 2 & 1 \\ -2 & -1 & 1 & 2 \end{bmatrix} \quad (16)$$

$$\begin{aligned} A^e_{11} &= \lambda (9,3,1,3) \, I^e \\ A^e_{12} &= A^e_{21} = \lambda (3,3,1,1) \, I^e \\ A^e_{13} &= A^e_{31} = A^e_{24} = A^e_{42} = \lambda (1,1,1,1) \, I^e \\ A^e_{14} &= A^e_{41} = \lambda (3,1,1,3) \, I^e \\ A^e_{22} &= \lambda (3,9,3,1) \, I^e \\ A^e_{23} &= A^e_{32} = \lambda (1,3,3,1) \, I^e \\ A^e_{33} &= \lambda (1,3,9,3) \, I^e \\ A^e_{34} &= A^e_{43} = \lambda (1,1,3,3) \, I^e \\ A^e_{44} &= \lambda (3,1,3,9) \, I^e \end{aligned} \quad (17)$$

where $\lambda = \frac{\Delta x \Delta y}{144}$, and I^e is the element vector of nodal values for the infectives. There are similar expressions for B^e_{ij} with I^e replaced by S^e the element vector of nodal values for the susceptibles.

After assembling the contributions from all elements we have

$$\left[\frac{1}{\Delta t} C - \frac{1}{2}(1-b) B + \frac{r}{2} C + bA + \frac{1}{2}(D+E)\right] \Delta I = \left[(1-b) B + \frac{1}{2}(1-b) \Delta B - rC - bA - (D+E)\right] I \quad (18)$$

where I is the vector of all nodal values for the infectives. In this equation C, D, E are constant matrices which need only be assembled once during the initiation process, while the matrices A, B and ΔB depend upon the instantaneous values of S^e and I^e and so must be reassembled for each time step.

At time level $t = n\Delta t$ we identify $I = I^n$ and $S = S^n$ and determine the updated nodal values from

$$I^{n+1} = I^n + \Delta I. \quad (19)$$

When we have prescribed the initial state of the system I^0 and S^0 the progress of the disease through the fox population can be modelled by successively applying Eqns. (6), (7) and (18), (19) and monitoring the values of S^n and I^n.

In the next sections we will first validate these equations and subsequently use them to simulate the spread of rabies over a rectangular region which approximates quite well the Isle of Anglesey.

Validation Studies

In earlier simulations [14–17] which satisfactorily reproduced field data on 4 measured quantities namely, speed of the infected pulse (30–60 km/yr), post epidemic susceptible minimum (~20%), endemic level (3–7%), and period of recurrence when the disease has entered the endemic phase (3–4 yrs), we chose the normalized birth and death rates to have values $b = 0.022$ and $r = 0.456$. These values were also used in the present work.

The simulation region used in the validation studies, measuring 163 km × 3.26 km, is large enough to exhibit all the salient features of the European epidemic. It was mapped by a mesh of 200 square elements of side $\Delta x = \Delta y = 1.0$ with 100 elements in the y direction and 2 in the x direction and the time step taken as $\Delta t = 0.333$. The scaling

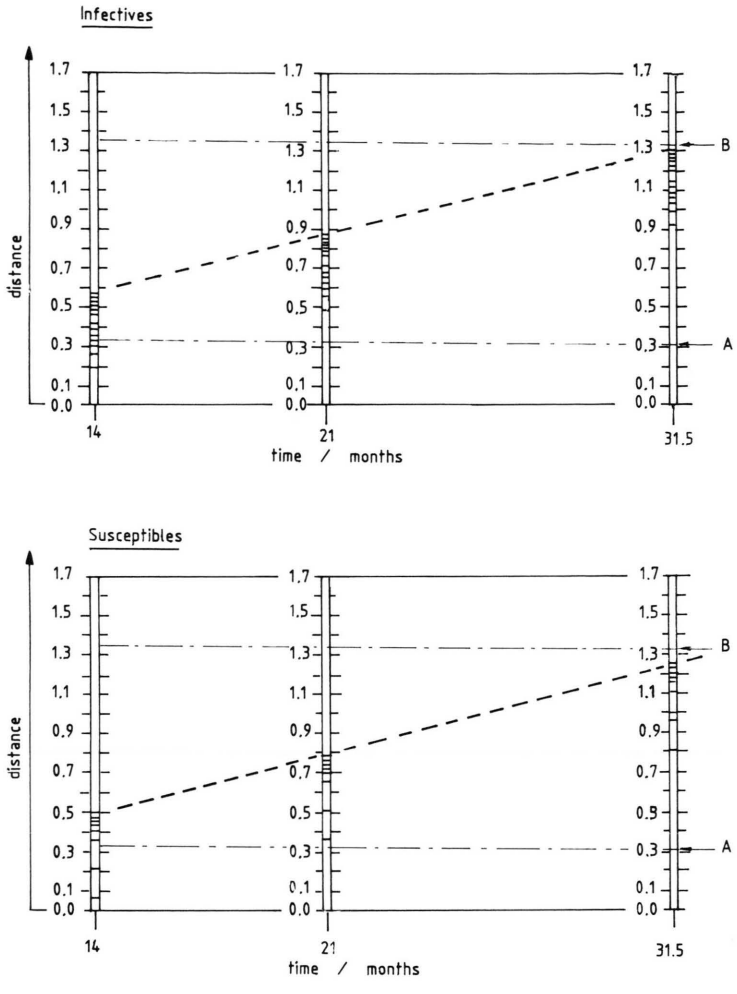

Fig. 1. Validation run. Rabies is introduced at the bottom of the region and progresses upwards. The leading edge of the infective pulse is marked by dotted line. Sampling points A and B are indicated. For the susceptibles: in front of the leading contour line the density is 1.0, and behind the last contour line the density has fallen to 0.2.

is such that distances in km = $1.63x$ or km = $1.63y$, time in years = $0.0437t$ so that velocity v in km/yr = $37.29v$; x, y, t and v are computational quantities. We examined the progress of the disease through a region with uniform initial density of susceptibles, at the carrying capacity of the region assumed uniform and constant (1.0), when introduced at all nodes along the end $x = 0$. This boundary condition satisfactorily reproduces the initial conditions used in the one-dimensional studies in which the disease was introduced at one end and its spread along the region monitored. The actual quantity of initial infection used (~10%) is unimportant as this governs only the length of the transient period during which the infective density at the initial site builds to a value of ~20%, while the susceptible density falls to a similar value. Thereafter the infective pulse where the disease is raging, delimited by the contour lines in Fig. 1, has width 40 km and a maximum magnitude of about 20%. The pulse travels across the region at a uniform speed of 51 km/yr eating into the susceptible population which is drastically reduced in density. On reaching the far end of the region the infective pulse would be expected to reflect but instead apparently disappears as the population of susceptibles is then too small to sustain the epidemic. Of course, the disease has not disappeared, but exists at a very low level throughout the entire region. At much later times after the fox population has regenerated itself to a level high enough to again sustain an infection, and this happens firstly

at the site of introduction from where further smaller pulses of infection radiate along the region causing dramatic falls in the size of the fox population. The time history of the population states at a single fixed sampling point are shown in Fig. 2. These results are typical of sites lying within the central field of the region.

We note that the infective pulse reaches this sampling point, at time $t = 55$, after ~165 time steps. Simultaneously the susceptible density falls rapidly to a minimum of ~20% and subsequently the disease dies away rapidly and apparently disappears from the neighbourhood of this sampling point. The fox population then regenerates itself and there are later outbreaks of the disease which again reduce the population resulting in an oscillation on the population density at this point. At later times the magnitude of these oscillations gradually decreases until a stable state is reached in which the disease is endemic at a very low but constant level in a population that has a reduced but constant density: this state has not been reached in Fig. 2. Decaying amplitudes are a feature of recurrent epidemics in models of this type [20].

In Fig. 3 we compare the times of arrival of the infective pulses at two sampling points A and B lying along the central line of the region a distance 60 Δx apart. We notice that the behaviour at each point is similar, that at the farthest point B from the initialization site being delayed over that at the nearer site A by about 120 Δt. The velocity of the pulse can be deduced from this figure. It is, however, more accurate to interrogate the computer code directly when we find that the velocity is 51.3 km/yr.

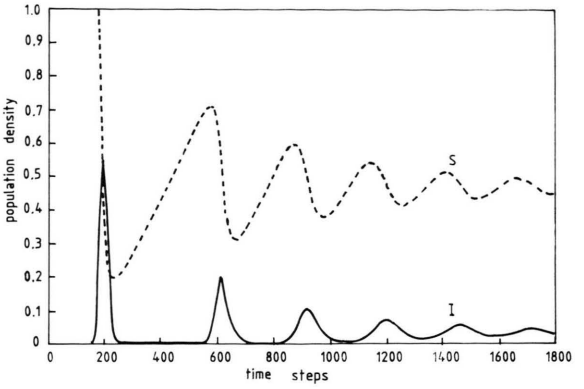

Fig. 2. Validation run. The evolution of the susceptible (S) and infective (I) densities at the fixed sampling point (B) in the centre of the region is shown. The graph of infective density has density values × 3 for clarity of presentation. $\Delta t = 0.333$.

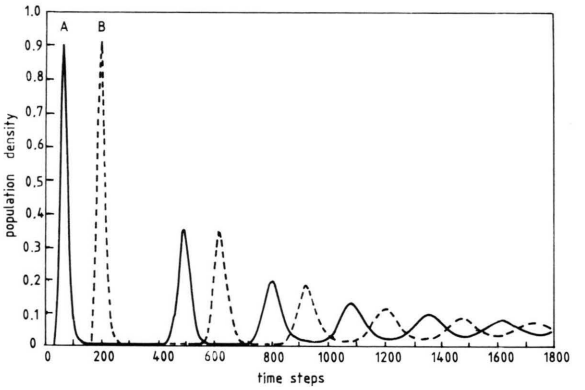

Fig. 3. Validation run. The state of infection (× 5), at sampling points A and B a distance 60 elements apart along the centre line of the region, is compared as a function of time. $\Delta t = 0.333$, $\Delta x = 1.0$.

Table I. Characteristic parameters from the simulations compared with theoretical and field data.

			Simulations			
	Theory [14]	Field data [11]	Finite diff. 1 D [14]	Finite element 1 D [16]	Hybrid Code 2 D [17]	Space time 2 D
Pulse speed [km/yr]	54	30–60	46	51	51	51
Post-epidemic S minimum [%]	≥15	20	19	18	18	20
$\frac{100 \times I}{(I+S)}$ %	2.3	3–7	2.4	2.3	2.3	2.4
Period [years]	3.8	3–4	3.8	4	3.8	3.9

From the graphs given in Fig. 2 and 3 estimates of all the characteristic quantities described earlier can be made. The values deduced are listed in Table I where they are compared with measurements made in our earlier simulations [14–17], with theoretical predictions [14], and field observations of the European epidemic [11]. The 1 D finite element results quoted in Table I are from a much longer simulation than that reported earlier [16] and consequently the endemic levels are more accurately described, and in fact reflect exactly the theoretical result. All characteristic values measured in this 2 D simulation are consistent with values published earlier. We thus feel completely justified in using the model to study the two-dimensional spread of rabies as described in the next section.

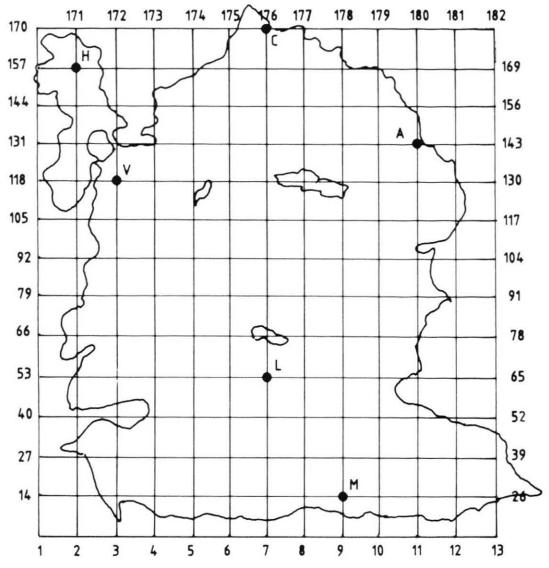

Fig. 4. A map of Anglesey showing its division into 12 × 13 finite elements each 2.5 km square. Node numbers and sampling points are shown.

Simultations

Off the North West coast of Wales lies the Isle of Anglesey, connected to the mainland by two bridges (the Menai and Britannia bridges) sited very close to one another. Due to the shape and orientation of the island it can be closely approximated within a rectangular region with parallel sides running approximately NE, NW. The bridges, mentioned above, and the Port of Holyhead provide the most probable entry sites for a rabies epidemic.

In these studies the rectangular simulation area was taken to be 30 × 32.5 km in size. This region was divided into 12 × 13 finite elements each 2.5 km square (see Fig. 4). The initial population of foxes was taken as uniform throughout the island (1 fox/km^2) with birth and death rates of $b = 0.022$, $r = 0.456$, consistent with parameters deduced earlier from European data on the epidemiology of rabies [14, 15]. The computational parameters were $dx = dy = 1.532$, $dt = 0.2$. The island is so small that the standard infective pulse, width ~40 km, would completely cover it, and so we cannot expect all the travelling wave features of the disease, apparent in a larger region, to be manifest. In the 2 cases studied here we have taken the initial sites of infection to be either near the centre of the lower side, which approximates to the position of the bridges joining Anglesey to the North Wales mainland, or near to the top left hand corner where the port of Holyhead is to be found. The spread of the disease from these sites has been examined and the initial transient state and the state in succeeding years evaluated. Sampling stations are indicated on Fig. 4 M-Menai Bridge, L-Llangefni, V-Valley, H-Holyhead, A-Amlwch, C-Carmel Head. Holyhead lies on a smaller island (Holy island) connected to the main island of Anglesey by a causeway and a bridge. This bottle neck will, as we shall see, influence the behaviour of the epidemic in the region of Holyhead.

Case (i)

Rabies introduced *via* the Menai Bridge. Computations show that the disease spreads rapidly northwards in a roughly symmetric manner reaching the north coast in about 8 months, contour lines showing the density distribution of infected and susceptible foxes at about 8.4 months into the epidemic are given in Fig. 5. The maximum of the infective pulse (~14%) reaches the northern shore in 10 months and at that time the fox population throughout the island has been reduced to a level of between 30–50% of its original value, although, because of access difficulties, the fox density around Holyhead has not fallen lower than 90%. The disease is endemic in the fox population which is now, in the main, so sparse as to be unable to sustain a vigorous epidemic.

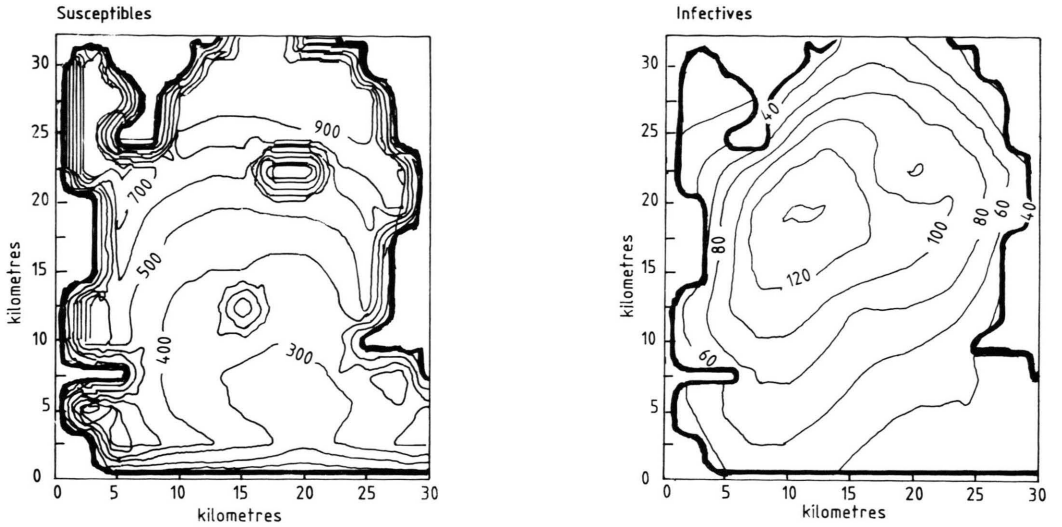

Fig. 5. Contour lines showing the density distribution (× 1000) of susceptible and infective fox population over Anglesey about 8.4 months after the infection was introduced *via* the Menai Bridge.

If we examine the state of the fox populations at a fixed site in the centre of the island, L – Llangefni, we obtain the graphs of susceptible and infective fox densities shown in Fig. 6.

Initially the susceptible density is 1.0; when the disease reaches the sampling point the susceptible density falls as the infected density increases. When the infective density attains its maximum of about 14%, the susceptible population has been reduced to about 60%. The susceptible population is then too small to sustain the epidemic at this site and as the susceptible density falls further to about 25% the infected density also falls away apparently to zero. The state of the disease over long periods is shown in Fig. 7. The recurrent phase of disease is evident and the period in the endemic state with an endemic level of 1.9% can be calculated as 3.9 years. Since the island is so small, the standard

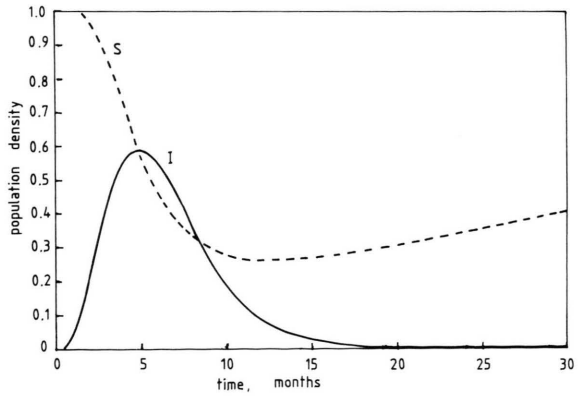

Fig. 6. The time evolution of the susceptible and infective fox densities at the sampling station L-Llangefni. Infective density (*I*) is plotted ×3 for clarity. Infection introduced over the Menai Bridge.

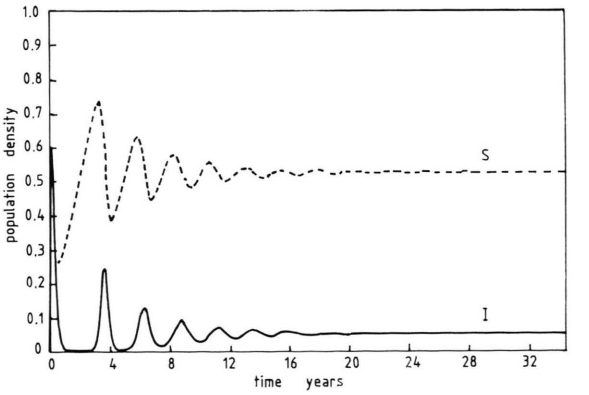

Fig. 7. The long-term evolution of the rabies infection at the sampling station L-Llangefni. Infection introduced *via* the Menai Bridge. Infective density (*I*) is plotted ×3 for clarity.

sized infective pulse does not develop, but most of the features of the progress of the disease described in the previous section are observed, albeit, at a reduced level. The fox population increases by natural growth until it reaches such a size as to be able to maintain an epidemic once more, at which time an infective pulse, smaller in magnitude than the original one, arises at the initial site (the Menai Bridge) and travels once more northwards across the island. This process is repeated again and again in following years.

At the other sampling stations similar behaviour is observed with identical endemic periods, but with final constant endemic levels of susceptibles S_∞ and infectives I_∞ of differing magnitudes. We find at M-Menai Bridge $S_\infty = 60\%$, $I_\infty = 0.8\%$, at L-Llangefni $S_\infty = 52\%$, $I_\infty = 1\%$, at V-Valley $S_\infty = 69\%$, $I_\infty = 0.6\%$, at H-Holyhead $S_\infty = 87\%$, $I_\infty = 0.3\%$, at A-Amlwch $S_\infty = 66\%$, $I_\infty = 0.7\%$ while at C-Carmel Head $S_\infty = 59\%$, $I_\infty = 0.9\%$.

The anomalous values at H-Holyhead arise because of the difficult access for diseased animals. In fact the variations between the sampling stations is probably caused by edge effects due to the small size of the island and its irregular boundary. Such non-uniformity was not observed with the previous model [17] which made no attempt to approximate the boundaries.

Case (ii)

Rabies introduced through Holyhead. Within 2 months the disease has leaked across the causeway and bridge linking Holy island to Anglesey proper. Now the disease radiates across Anglesey in a south easterly direction the wave front reaching the south coast in about 9 months and the crest of the pulse in about 14 months. Contours of population density about 8.4 months into the epidemic for sampling station L-Langefni are given in Fig. 8. Eventually the fox population throughout the Island is reduced to about 30%. In subsequent years pulses of disease travel south eastwards from Holyhead across the Island as the fox population regenerates itself and is once more decimated by the disease.

We have examined the state of the fox population using the sampling stations previously detailed. The time development of the epidemic at L-Langefni is shown in Fig. 9. The graphs obtained are very similar to those given previously for L-Llangefni, Fig. 6, when the disease was introduced at Menai Bridge.

In fact, in this second case the long term results for all sampling stations present a more uniform picture, apart from those for V-Valley and H-Holyhead which are influenced considerably by

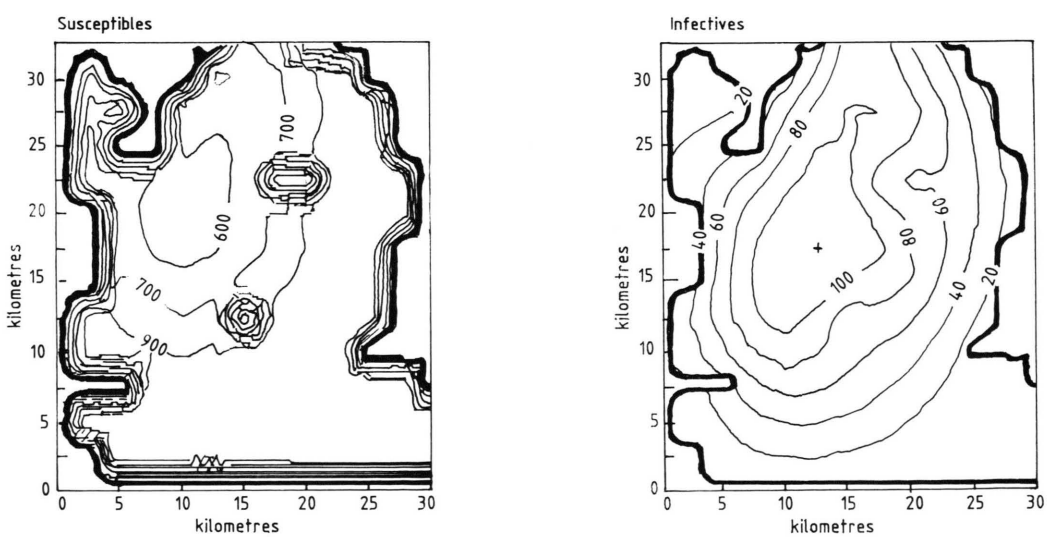

Fig. 8. Contour lines showing the density distribution (× 1000) of susceptible and infective fox population over Anglesey about 8.4 months after the infection was introduced through the port of Holyhead.

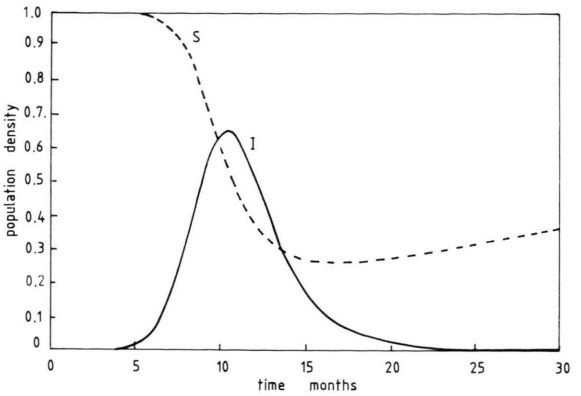

Fig. 9. The time evolution of the susceptible and infective fox densities at the sampling station L-Llangefni. Infection introduced through the port of Holyhead. *I* curve plotted × 3 for clarity.

the narrowness of the connecting links between Holy island and Anglesey proper.

Conclusions

The two-dimensional finite element method set up and described in this paper has been validated by comparing the results of simulations in a long thin two-dimensional region with earlier mainly one-dimensional results. The parameters we calculate are in full agreement with theoretical and experimental results. We have therefore confidence in using the method to study the spread of rabies in fully two-dimensional regions.

Our aim has been to develop codes which can be used with personal computers in the field in the likely event of rabies introduction to the U.K. We have chosen as a pilot study area, the Isle of Anglesey, a region adjacent to our University. We have modelled the spread of rabies over this island, approximating it within a rectangular region. Due to the shape of Anglesey this approximation is not expected to have a significant influence on the overall picture but will have local consequences. This island is so small that the results are considerably influenced by boundary effects. Nonetheless, most observations are fully consistent with expected disease characteristics. The computer code described here will, in future, be used in large scale simulations of irregular and inhomogeneous regions.

For many years there has been interest in stochastic models of the spatial spread of epidemics (see, for example, Mollison [21, 22]) but since such models are often intractable they have not been developed to any great extent and have been little used in biology. In our study it is clear, from Fig. 2 for example, that infective fox densities in the immediate aftermath of the initial epidemic pulse are very small indeed; also in control studies extinction of infectives is the objective [14] and the study of small densities is essential. If, deterministically, in a single fox territory the infective density is very small (corresponding to a tiny fraction of a fox) it is logical to deem that extinction of infectives has occurred in that territory; in other words densities should be cut off at some level. However, in propagation studies, as described in this paper, many territories are chained together and a very small infective density could represent a single rabid fox in some territory (a source for a recurrent outbreak) with rabies extinct almost everywhere; then it is not obvious that small densities should be cut off. Moreover, in situations such as exist in some English cities much higher fox densities than those considered here are reported (see Harris [23]) and rabies epidemics in these conditions may devastate the entire fox population requiring study of small susceptible densities also [24]. The case for a stochastic study is therefore very strong. The present authors have made preliminary studies of the problem in relation to fox rabies [25, 26] and expect, at a later date, to publish the results of a detailed study.

[1] G. M. Baer, The Natural History of Rabies, **Vol. I, II,** Academic Press, New York 1975.
[2] P. K. Sykes, Am. J. Vet. Res. **23,** 1041–1047 (1962).
[3] R. L. Parker and R. E. Wilnack, Am. J. Vet. Res. **27,** 33–46 (1966).
[4] D. G. Constantine, Am. J. Vet. Res. **27,** 13–32 (1966).
[5] C. Kaplin (ed.), Rabies: The Facts, Oxford University Press, Oxford 1977.
[6] F. Fenner, B. R. McAuslan, C. A. Mims, J. Sambrook, and P. O. White, The Biology of Animal Viruses, Academic Press, New York 1974.
[7] Wld. Hlth. Orgn., Rabies Bulletin Europe **3,** 5, WHO Centre for Rabies Surveillance and Research, Tübingen (1980).
[8] D. W. MacDonald, R. G. H. Bunce, and P. J. Bacon, J. Biogeography **8,** 145–151 (1981).
[9] D. W. MacDonald, Rabies and Wildlife, A Biologists Perspective, Oxford University Press, Oxford 1980.
[10] N. T. J. Bailey, The Mathematical Theory of Infectious Diseases and Applications, Griffin Press, London 1975.
[11] R. M. Anderson, H. C. Jackson, R. M. May, and A. M. Smith, Nature **289,** 765–771 (1981).
[12] A. Källén, P. Arcuri, and J. D. Murray, J. Theor. Biol. **116,** 377–393 (1985).
[13] J. D. Murray, E. A. Stanley, and D. L. Brown, Proc. Roy. Soc. **229,** 111–150 (1986).
[14] J. Cunningham, L. R. T. Gardner, G. A. Gardner, and H. A. Shaoul, Epidemiology of Rabies in a Logistic Population, Proc. Inter. Conf. on Modelling and Simulations, Sorrento 1986, **4.2,** 3–12, AMSE Press, Tassin-la-Demi-Lune, France 1986.
[15] J. Cunningham, L. R. T. Gardner, and G. A. Gardner, Effects of Latency and Seasonality on the Spatial Spread of Rabies in a Logistic Fox Population, Proc. Inter. Conf. on Modelling and Simulations, Karlsruhe 1987, **4,** 25–36, AMSE Press, Tassin-la-Demi-Lune, France 1987.
[16] L. R. T. Gardner, G. A. Gardner, J. Cunningham, and A. Kanawati, A Finite Element Model for the Spatial Spread of Rabies, Proc. Inter. Conf. on Modelling and Simulations, Karlsruhe 1987, **4,** 13–24, AMSE Press, Tassin-la-Demi-Lune, France 1987.
[17] G. A. Gardner, L. R. T. Gardner, and J. Cunningham, A Finite Element Model for the Two-Dimensional Spread of Rabies, Proc. Inter. Conf. on Modelling and Simulations, Istanbul 1988, **4A,** 11–25, AMSE Press, Tassin-la-Demi-Lune, France 1988.
[18] O. C. Zienkiewicz, The Finite Element Method, McGraw Hill, London (3rd Edition) 1977.
[19] A. C. Hearn, REDUCE Users Manual Version 3.2, Northwest Computer Algorithms 1986.
[20] J. Cunningham, Z. Naturforsch. **34c,** 647–648 (1979).
[21] D. Mollison, J. Roy. Stat. Soc. B **39,** 397–426 (1977).
[22] D. Mollison, Phil. Trans. Roy. Soc. Lond. B **314,** 675–693 (1986).
[23] S. Harris, Urban Foxes, Whittet Books, London 1986.
[24] J. Cunningham, G. A. Gardner, and L. R. T. Gardner, Some Consequences of Vector Density Variation on the Spatial Spread of Rabies, UCNW Maths Preprint 90.17 (1990).
[25] J. Cunningham, G. A. Gardner, and L. R. T. Gardner, Stochastic Simulations of Rabies Spread, Proc. Inter. Conf. on Signals and Systems, Rabat 1990, **2,** 191–199, AMSE Press, Tassin-la-Demi-Lune, France 1990.
[26] J. Cunningham, G. A. Gardner, and L. R. T. Gardner, Pseudo-Stochastic Simulations of Rabies Spread, Proc. Inter. Conf. on Signals and Systems, Rabat 1990, **2,** 201–211, AMSE Press, Tassin-la-Demi-Lune, France 1990.